Comparison of two forward solutions approaches in Lorentz Force Evaluation

E.-M. Dölker[1], R. Schmidt[2], K. Weise[2], B. Petković[1], M. Ziolkowski[2], H. Brauer[2], and Jens Haueisen[1]

[1]Institute of Biomedical Engineering and Informatics, Technische Universität Ilmenau, Ilmenau, 98693, Germany, eva-maria.doelker@tu-ilmenau.de
[2]Advanced Electromagnetics Group, Technische Universität Ilmenau, Ilmenau, 98693, Germany, reinhard.schmidt@tu-ilmenau.de

Two different forward models for Lorentz force evaluation, the approximate forward solution (AFS) and the novel extended area approach (EAA), are compared using a goal function scan. A laminated aluminum specimen that contains a cuboidal defect of the size 12 mm x 2 mm x 2 mm at 2 mm depth is simulated by the finite element method. Both methods are applied for defect reconstruction and showed a correct depth estimation with normalized root mean square errors (*NRMSE*) of 6.05 % for AFS and 1.67 % for EAA, respectively. The EAA yields defect dimensions of 11 mm x 2 mm x 2 mm, whereas AFS determines 7 mm x 10 mm x 2 mm.

***Index Terms*—Eddy current, Lorentz force evaluation, inverse problem, nondestructive evaluation**

I. Introduction

The Lorentz force evaluation (LFE) is a nondestructive method, which reconstructs defects from perturbations in Lorentz forces that act on a permanent magnet, which moves relatively to a conductive specimen. Previous defect reconstructions have been performed by truncated singular value decomposition [1], differential evolution [2] and current density reconstruction [3], where all were based on the approximate forward solution (AFS) [1]. Recently, the more accurate extended area approach (EAA) has been introduced as forward model for LFE [4]. It is the aim of the current study to compare the performance of AFS and the novel EAA with regard to defect reconstruction performance. For that purpose, a goal function scan [5] is applied to a simulated dataset obtained by the finite element method (FEM), which is used for modeling a specimen consisting of stacked aluminum sheets and a cuboidal defect.

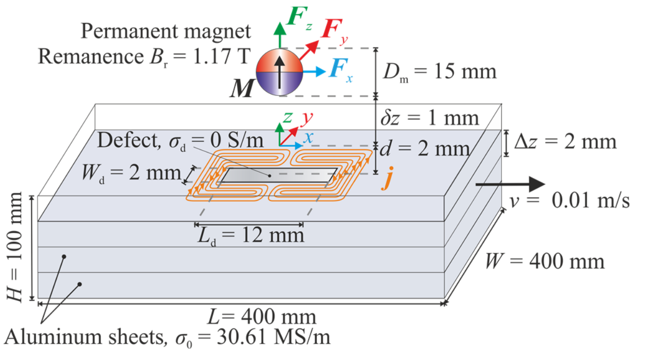

Fig. 1. Benchmark problem: A package of aluminum sheets with a cuboidal defect is moved relatively to the spherical permanent magnet, where the interaction of the induced eddy currents (orange lines) with the magnetic field leads to Lorentz forces; the figure is not to scale for better visualization.

II. Methods

A. Benchmark problem

A specimen with $L \times W \times H = 400\text{ mm} \times 400\text{ mm} \times 100\text{ mm}$ and the conductivity $\sigma_0 = 30.61\text{ MS/m}$ is moved relatively to the permanent magnet with the velocity $v = 0.01\text{ m/s}$ (Fig. 1). Due to the relative movement eddy currents are induced, where the interaction with the magnetic field leads to Lorentz forces. In presence of a defect these eddy currents are perturbed (Fig. 1) and so are the Lorentz forces. The specimen consists of stacked aluminum sheets, where each sheet possesses a thickness of $\Delta z = 2\text{ mm}$. The spherical permanent magnet with the homogenous magnetization $\boldsymbol{M}$ is located at the lift-off distance $\delta z = 1\text{ mm}$ above the top surface of the specimen. It is characterized by a remanence of $B_r = 1.17\text{ T}$ and a diameter $D_\mathrm{m} = 15\text{ mm}$. A cuboidal defect with the conductivity $\sigma_\mathrm{d} = 0\text{ S/m}$ and $L_\mathrm{d} \times W_\mathrm{d} \times H_\mathrm{d} = 12\text{ mm} \times 2\text{ mm} \times 2\text{ mm}$ is located at the depth $d = 2\text{ mm}$.

B. Approximate Forward Solution and Extended Area Approach

The spherical permanent magnet is modelled as a magnetic dipole located at its center $\boldsymbol{r}_0$. The magnetic flux density at the point $\boldsymbol{r}$ can be calculated by

$$\boldsymbol{B}_\mathrm{p} = \frac{\mu_0}{4\pi}\left(3\frac{[\boldsymbol{m}\cdot(\boldsymbol{r}-\boldsymbol{r}_0)]}{|\boldsymbol{r}-\boldsymbol{r}_0|^5}(\boldsymbol{r}-\boldsymbol{r}_0) - \frac{\boldsymbol{m}}{|\boldsymbol{r}-\boldsymbol{r}_0|^3}\right), \tag{1}$$

where $\boldsymbol{m}$ denotes the magnetic moment. Due to the small velocity $\boldsymbol{v}$, the secondary magnetic field from the induced eddy currents can be neglected. Thus, the weak reaction approach can be applied [6].

The defect response signal (DRS) $\Delta\boldsymbol{F}$ [4], which forms the basis for the defect reconstruction is defined by

$$\Delta\boldsymbol{F} = \underbrace{\int_{V-V_\mathrm{d}} (\boldsymbol{j}-\boldsymbol{j}_0)\times\boldsymbol{B}_\mathrm{p}\,dV - \underbrace{\int_{V_\mathrm{d}} \boldsymbol{j}_0\times\boldsymbol{B}_\mathrm{p}\,dV}_{\text{AFS}}}_{\text{EAA}}, \tag{2}$$

where $\boldsymbol{j}$ and $\boldsymbol{j}_0$ represent the current density in the specimen with and without a defect, respectively. The volumes of the specimen and the defect are denoted by V and V_d.

The AFS neglects the first term of (2), which means that only the defect as a fictitious conducting region is taken into account for the calculation of the DRS. The defect is discretized into K volume elements (voxels) of volume V_{E}. The DRS is then approximated by [1]

$$\Delta \boldsymbol{F}_{\mathrm{AFS}} = V_{\mathrm{E}} \sum_{k=1}^{K} \Delta \boldsymbol{j}_k \times \boldsymbol{B}_k \ . \tag{3}$$

The distortion current density $\Delta \boldsymbol{j}_k = -\boldsymbol{j}_0$ can be calculated by Ohm's law for moving conductors $\Delta \boldsymbol{j}_k = -\sigma_0\left(-\nabla \varphi_k + \boldsymbol{v} \times \boldsymbol{B}_k\right)$ [1], where $\boldsymbol{B}_k$ denotes the magnetic flux densities inside the voxels. The EAA extends the region for forward calculation in $x-$ and $y-$ direction around the defect, which approximates the first term of (2). The extended area is discretized into E cuboidal voxels. Thus $\Delta \boldsymbol{F}$ is approximated by [4]

$$\Delta \boldsymbol{F}_{\mathrm{EAA}} = V_{\mathrm{E}} \sum_{e=1}^{E} \Delta \boldsymbol{j}_e \times \boldsymbol{B}_e + \Delta \boldsymbol{F}_{\mathrm{AFS}} , \tag{4}$$

where the magnetic flux densities inside the extended voxels are denoted by $\boldsymbol{B}_e$. The distortion current densities $\Delta \boldsymbol{j}_e$ in the outer voxels can be determined by [4]

$$\Delta \boldsymbol{j}_e \cong C_{\mathrm{d}} \frac{V_{\mathrm{E}}}{2\pi \Delta z} \sum_{k=1}^{K} \left[2 \frac{\Delta \boldsymbol{j}_k \cdot (\boldsymbol{r}_e - \boldsymbol{r}_k)}{\left|\boldsymbol{r}_e - \boldsymbol{r}_k\right|^4} (\boldsymbol{r}_e - \boldsymbol{r}_k) - \frac{\Delta \boldsymbol{j}_k}{\left|\boldsymbol{r}_e - \boldsymbol{r}_k\right|^2} \right], \tag{5}$$

where the dipolar correction factor $C_{\mathrm{d}} = 1 + (\pi/4)(L_{\mathrm{d}}/W_{\mathrm{d}})$ holds for cuboidal defects [4]. The position vectors of the voxels' centroids in the defect and the extended region are denoted by $\boldsymbol{r}_k$ and $\boldsymbol{r}_e$, respectively.

For the EAA, the decision of an appropriate expansion size is important. The DRS $\Delta \boldsymbol{F}_{\mathrm{EAA}}$ is calculated for the benchmark problem for the extensions $ex = [0, 1, 2, \ldots, 7] \cdot \max(L_{\mathrm{d}}, W_{\mathrm{d}})$ in $\pm x-$ and $y-$direction, where 0 means AFS is applied. The expansion has been chosen to $ex = 5 \cdot \max(W_{\mathrm{d}}, L_{\mathrm{d}})$ as the adapted normalized root mean square error (*aNRMSE*)—stopped improving.

C. Goal Function Scan

The DRS is calculated by AFS according to (3) and by EAA according to (4), respectively, for the combinations of $L_{\mathrm{d}} = [1, 2, ..., 50\ \mathrm{mm}]$ and $W_{\mathrm{d}} = [1, 2, ..., 50\ \mathrm{mm}]$ from the 1st to the 11th layer. For each calculation, the *aNRMSE* is determined as a goal function value by

$$aNRMSE = \frac{1}{2} \sum_{i=x,z} \left[\frac{\sqrt{\frac{1}{N} \sum_{n=1}^{N} \left(\Delta F_{n,i}^{\mathrm{AFS/EAA}} - \Delta F_{n,i}^{\mathrm{FEM}}\right)^2}}{\min\left[\left(\max\limits_{n=1...N} \Delta \boldsymbol{F}_i^{\mathrm{AFS/EAA}} - \min\limits_{n=1...N} \Delta \boldsymbol{F}_i^{\mathrm{AFS/EAA}}\right), \left(\max\limits_{n=1...N} \Delta \boldsymbol{F}_i^{\mathrm{FEM}} - \min\limits_{n=1...N} \Delta \boldsymbol{F}_i^{\mathrm{FEM}}\right)\right]} \right], \tag{6}$$

where n indicates the current position of the magnetic dipole. Only the $x-$and $z-$error components are used since the $y-$component of the DRS shows too large errors for both forward models. For every aluminum layer, the $L_{\mathrm{d}} - W_{\mathrm{d}}$-combination with the lowest *aNRMSE* is determined for AFS and EAA. The layer with the lowest *aNRMSE* gives the result for the depth and the size of the defect produced by the goal function scan for AFS and EAA.

III. Results and Discussion

Fig. 2 shows the *aNRMSE* and the corresponding estimated defect extensions $L_{\mathrm{d}} \times W_{\mathrm{d}}$ in $x-$ and $y-$ direction in mm² (indices, Fig.2) over the aluminum layers for AFS and EAA. It can be observed that both methods determine the defect depth at layer 2 correctly, whereas AFS reconstructs a size of $7\ \mathrm{mm} \times 10\ \mathrm{mm} \times 2\ \mathrm{mm}$ and EAA of $11\ \mathrm{mm} \times 2\ \mathrm{mm} \times 2\ \mathrm{mm}$, respectively.

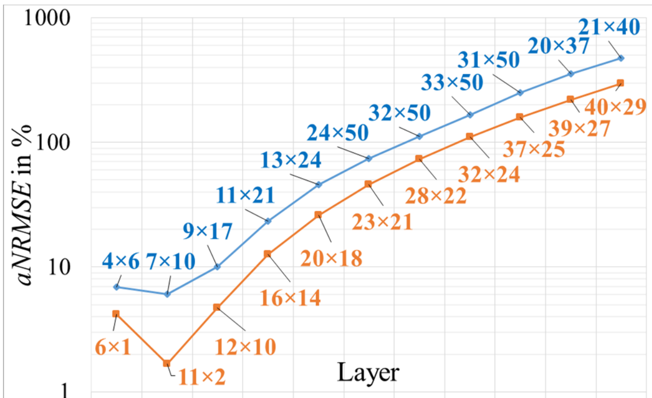

	1	2	3	4	5	6	7	8	9	10	11
AFS	7	6	10	23	46	74	111	166	250	357	478
EAA	4	2	5	13	26	46	73	110	159	220	298

Fig. 2. Results of the goal function scan based on AFS and EAA for a cuboidal defect with $x-y-$ extension (12×2) mm² at the depth 2 mm: The minimal *aNRMSE* and its corresponding estimated defect extension ($L_{\mathrm{d}} \times W_{\mathrm{d}}$) mm² are shown for each layer. The correct defect depth (layer 2) has been found for both forward solutions, whereas the EAA estimates the defect shape more accurately. The rounded *aNRMSE* values are shown in the table.

IV. Conclusion

The comparison of AFS and EAA for LFE based on a goal function scan shows that correct defect depth can be estimated with both methods, whereas a better shape reconstruction can be achieved by using the EAA. Current work focuses on the application of the EAA to measurement data.

References

[1] B. Petković, J. Haueisen, M. Zec, R. P. Uhlig, H. Brauer and M. Ziolkowski. Lorentz force evaluation: A new approximation method for defect reconstruction. NDT & E International, vol. 59, pp. 57–67, 2013.

[2] J. Mengelkamp, D. Lattner, J. Haueisen, M. Carlstedt, K. Weise, H. Brauer, M. Ziolkowski and R. Eichardt. Lorentz force evaluation with differential evolution. IEEE Transactions on Magnetics, vol. 52, no. 5, pp. 6201310 (1-10), 2016.

[3] J. Mengelkamp, M. Carlstedt, K. Weise, M. Ziolkowski, H. Brauer and J. Haueisen. Current density reconstructions for Lorentz force evaluation. Research in Nondestructive Evaluation, pp. 1-25, 2016.

[4] M. Ziolkowski, Modern methods for electromagnetic field problems. Szczecin, Poland: West Pomeranian University of Technology College Publisher, 2015.

[5] J. C. Mosher, P. S. Lewis and R. M. Leahy. Multiple dipole modeling and localization from spatio-temporal MEG data. IEEE Transactions on Biomedical Engineering., vol. 39, no. 6, pp. 541-557, 1992.

[6] M. Zec, R. P. Uhlig, M. Ziolkowski and H. Brauer, Fast technique for Lorentz force calculations in nondestructive testing applications, IEEE Transactions on Magnetics, vol. 50, no. 2, pp. 7003104 (1-4), 2014.